Quantum theory of a semiconductor klystron

Masahiro Asada*
Interdisciplinary Graduate School of Science and Engineering, Tokyo Institute of Technology, 2-12-1 O-okayama, Meguro-Ku, Tokyo 152-8552, Japan
(Received 8 October 2002; published 3 March 2003)

The interaction between a hot electron beam and electromagnetic waves is analyzed in a semiconductor with the structure of the klystron device, in which electrons emit or absorb photons at the input port and then make a spontaneous emission at the output port. As a result of the collective spontaneous emission due to the interference between the specific many-electron states, the output photons have harmonic frequencies of the input, and the emission rate is proportional to square of the beam current. Due to the influence of electron scattering, the output power is much reduced for an input photon energy smaller than the electron energy broadening determined by the scattering and also for an input-output interval larger than the electron coherence length.

DOI: 10.1103/PhysRevB.67.115303 PACS number(s): 78.67.−n, 73.63.−b, 78.70.Gq, 85.35.−p

I. INTRODUCTION

An analysis is shown in this paper for the interaction between hot electrons and electromagnetic (EM) waves in a semiconductor nanostructure corresponding to the klystron device which is a vacuum tube for the amplification of the microwave. The klystron consists of input and output ports for EM waves and an electron beam traversing them, the structure of which is the same as that shown later in Fig. 1 for the analysis, except that a semiconductor is supposed in Fig. 1 instead of the vacuum. The interaction of the electron beam with the EM waves in this vacuum tube has been analyzed classically,[1] in which the electron beam traversing the input port is accelerated or decelerated by the input electric field, and the charge density modulation occurs after the travel from the input to output ports. This modulated beam radiates an EM wave into the output port. In this process, a part of the electron kinetic energy is transferred to the output EM wave, resulting in amplification.

The electron beam responds to higher frequency as the traverse times at the input and output ports are reduced. Therefore, if the klystron is fabricated in a semiconductor nanostructure, a high-frequency response is expected, in spite of the fact that the electron energy is much lower than that in the vacuum klystron. As the frequency and thus the photon energy increase, a quantum-mechanical analysis and discussion of the deviation from the classical results become important. Also, the influence of various scattering mechanisms, such as electron-phonon and electron-electron scatterings, must be taken into account in high-density electron beams in a semiconductor nanostructure, in contrast to the vacuum.

In the classical analysis, the output EM wave has the harmonic frequency of the input, and the output power is proportional to square of the beam current, in agreement with the observation. The quantum-mechanical analysis must produce the same result at least in the low-frequency limit. Quantum mechanically the electron beam interacts with photons at the input port and then makes a spontaneous emission at the output port. However, these properties are quite different from those of conventional spontaneous emission which has no relation to the input frequency and is proportional to the electron density or current. Quantum-mechanical analyses for the radiation from a modulated electron beam in the vacuum have been reported,[2–5] where the collective spontaneous emission from the electron beam has been shown to have the above properties of the klystron.

In this paper, the interaction between electrons and photons in a semiconductor klystron structure is systematically analyzed for a relatively wide frequency range from microwave to far infrared, including the influence of electron scattering. In Sec. II, the analytical model and the output photon rate including the electron scattering are given. It is shown that the output photons have the harmonic frequencies of the input and the emission rate is proportional to the square of the beam current. A simple physical interpretation for these results is also given using the interference between the specific many-electron states. The influence of the scattering on the output power is discussed in Sec. III. The output power is much reduced for an input photon energy smaller than the electron energy broadening due to the scattering and also for an input-output interval larger than the electron coherence length. The classical limit and the output with no relation to the input frequency are also discussed.

II. ANALYSIS

A. Structure and Hamiltonian

The electron-photon interaction system discussed in this paper is shown in Fig. 1. A hot electron beam is supposed to flow in a semiconductor heterostructure with the input and output ports for EM waves. Each port is constructed, for

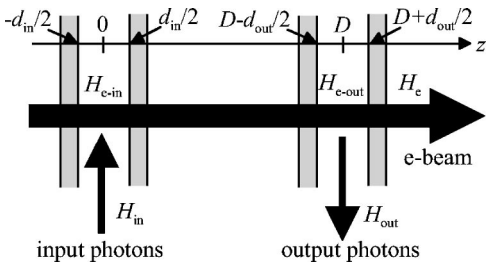

FIG. 1. Electron-photon interaction system in a semiconductor heterostructure discussed in this paper.

example, by a pair of parallel thin layers of metal or heavily doped semiconductor. The reflection of electron waves at the heterointerfaces is neglected in the analysis. The input EM wave traverses the electron beam, resulting in the absorption and stimulated emission. The output is generated up and downwards into the output port by spontaneous emission from the electron beam.

The Hamiltonian of the system is

$$H = H_e + H_{\text{in}} + H_{\text{out}} + H_{e\text{-in}} + H_{e\text{-out}}, \tag{1}$$

where H_e, H_{in}, and H_{out} are the Hamiltonians of the electron beam and input and output photons, respectively, given by

$$H_e = \sum_k \mathcal{E}_k c_k^\dagger c_k + H_{\text{scattering}}, \tag{2a}$$

$$H_{\text{in}} = \hbar\omega_{\text{in}} a_{\text{in}}^\dagger a_{\text{in}}, \tag{2b}$$

$$H_{\text{out}} = \hbar\omega_{\text{out}} a_{\text{out}}^\dagger a_{\text{out}}, \tag{2c}$$

where the subscript k in the electron system denotes the wave vector of an electron, which consists of compositions parallel ($k_\parallel$) and perpendicular (k_z) to the heterointerface, and $\mathcal{E}_k = \hbar^2 k_z^2/2m + \hbar^2 k_\parallel^2/2m = \mathcal{E}_z + \mathcal{E}_\parallel$ with electron effective mass m. Only one parabolic energy band is considered here. Various electron scatterings, such as electron-phonon and electron-electron scatterings, are expressed by $H_{\text{scattering}}$. The effect of the scatterings is considered as a change of the self-energy in the analysis shown below. Although only one mode is considered for simplicity in both the input and output photon systems in Eqs. (2b) and (2c), results for the multimode case are obtained by integrating those for the single mode.

$H_{e\text{-in}}$ and $H_{e\text{-out}}$ in Eq. (1) denote the interaction of the electron beam with the input and output photons, respectively. $H_{e\text{-in}}$ is given by

$$H_{e\text{-in}} = \sum_{kk'} c_k^\dagger c_{k'} \int_S \int_{-d_{\text{in}}/2}^{d_{\text{in}}/2} \frac{-ie\hbar}{2m} \psi_k^*(r)[\nabla \cdot A_{\text{in}}(r) + A_{\text{in}}(r)\cdot\nabla]\psi_{k'}(r)\,dz\,dS, \tag{3}$$

where d_{in} is the gap of the input port as shown in Fig. 1, $\psi_k(r) = e^{-ikr}/\sqrt{LS}$ is the electron envelope function with the length L along the z axis and the cross-sectional area S, and $A_{\text{in}}(r)$ is the vector potential given by

$$A_{\text{in}}(r) = \sqrt{\frac{\hbar}{2\varepsilon\omega_{\text{in}} W_{\text{in}} \ell_{\text{in}} d_{\text{in}}}}\,[a_{\text{in}}^\dagger F_{\text{in}}^*(r) + a_{\text{in}} F_{\text{in}}(r)]e_{\text{in}}, \tag{4}$$

where ε is the dielectric constant, W_{in} is the width of the input port perpendicular to the propagation directions of the electron beam and input EM wave, ℓ_{in} is the length of the input photon system along the propagation direction of the input EM wave, by which the photon number and the mode density of the system are defined [see Eqs. (29) and (30) below], the spatial distribution $F_{\text{in}}(r)$ is normalized so that the integral of the absolute square over the whole region of the input photon system is equal to the volume $W_{\text{in}}\ell_{\text{in}} d_{\text{in}}$, and e_{in} is the unit vector indicating the polarization direction.

Hereafter the TEM (transeverse electric and magnetic) mode is supposed for the input, in which e_{in} is in the z direction and $F_{\text{in}}(r)$ is uniform in the z direction. Further, the wavelength is assumed much longer than the cross-sectional size of the electron beam. By these assumptions, $F_{\text{in}}(r) \simeq 1$ in Eq. (4), and $H_{e\text{-in}}$ in Eq. (3) is calculated as

$$H_{e\text{-in}} = \sum_{k_\parallel k_z k_z'} M_{\text{in}}(k_z, k_z') c_k^\dagger c_{k'} (a_{\text{in}}^\dagger + a_{\text{in}}), \tag{5}$$

where the summation for $k_\parallel'$ is eliminated because $k_\parallel' = k_\parallel$ due to the above assumption, and

$$M_{\text{in}}(k_z, k_z') \simeq -\frac{e}{2}(v_z + v_z')\sqrt{\frac{\hbar d_{\text{in}}}{2\varepsilon\omega_{\text{in}} W_{\text{in}} \ell_{\text{in}}}}\frac{1}{L} \times M\left((k_z - k_z')\frac{d_{\text{in}}}{2}\right), \tag{6}$$

where $v_z = \hbar k_z/m$ is the electron velocity in the z direction, and $M(x) = \sin x/x$.

$H_{e\text{-out}}$ is obtained similarly as

$$H_{e\text{-out}} = \sum_{k_\parallel k_z k_z'} M_{\text{out}}(k_z, k_z') c_k^\dagger c_{k'} (a_{\text{out}}^\dagger + a_{\text{out}}). \tag{7}$$

$M_{\text{out}}(k_z, k_z')$ is given by changing the subscript "in" with "out" in Eq. (6) and multiplying the factor $e^{-i(k_z - k_z')D}$, where D is the interval between the centers of the input and ouput ports, as shown in Fig. 1.

B. Output photon rate

The rate of output photon number is given by

$$\left\langle \frac{dN_{\text{out}}}{dt} \right\rangle = \frac{1}{i\hbar} \sum_{k_\parallel k_z k_z'} M_{\text{out}}(k_z, k_z')\,\text{Tr}[\rho c_k^\dagger c_{k'} (a_{\text{out}}^\dagger - a_{\text{out}})]. \tag{8}$$

ρ is the density operator of the whole system given by

$$\rho = U(t, -\infty)(\bar{\rho}_e \otimes \bar{\rho}_{\text{in}} \otimes \bar{\rho}_{\text{out}}) U(-\infty, t), \tag{9}$$

where

$$U(t, t_0) = \exp[H(t - t_0)/i\hbar], \tag{10}$$

$$\bar{\rho}_{\text{in}} = |N_{\text{in}}\rangle\langle N_{\text{in}}|, \tag{11}$$

$$\bar{\rho}_{\text{out}} = |0\rangle_{\text{out}}\langle 0|_{\text{out}}, \tag{12}$$

$\bar{\rho}_e$ is the density operator of electron system without $H_{e\text{-in}}$ and $H_{e\text{-out}}$, N_{in} in Eq. (11) is the input photon number, and the initial output photon number is assumed to be zero in Eq. (12). Expanding ρ in Eq. (9) up to first order in $H_{e\text{-out}}$, the rate of output photon number is obtained as

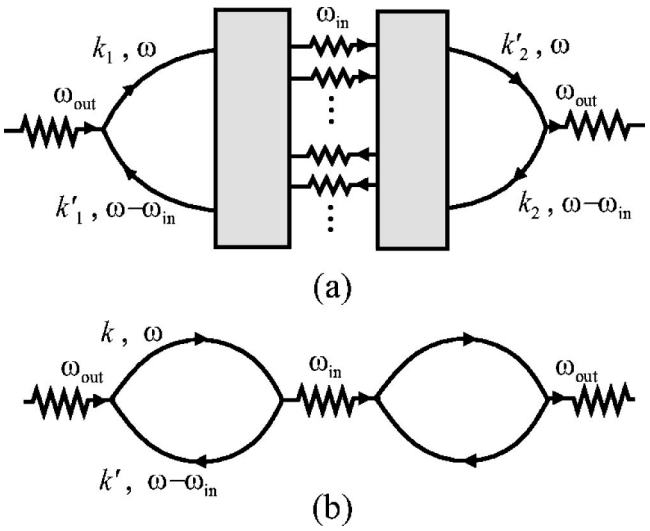

FIG. 2. Diagrams in which the output has a harmonic frequency of the input. The left and right parts are linked only by the input photon propagators. (a) General and (b) the lowest-order terms.

$$\left\langle \frac{dN_{\rm out}}{dt} \right\rangle = \frac{1}{\hbar^2} \sum_{k_{1\|}k_{2\|}} \sum_{k_{1z}k'_{1z}k_{2z}k'_{2z}} M_{\rm out}(k_{1z},k'_{1z}) \times M_{\rm out}(k_{2z},k'_{2z}) \int_{-\infty}^{\infty} {\rm Tr}[\overline{\rho_e} c^{\dagger}_{k_1}(t') c_{k'_1} \times (t') c^{\dagger}_{k_2}(0) c_{k'_2}(0)] e^{-i\omega_{\rm out}t'} dt', \tag{13}$$

where $c^{\dagger}_k(t) = U_{e\text{-in}}(-\infty,t) c^{\dagger}_k U_{\text{e-in}}(t,-\infty)$ with $U_{e\text{-in}}(t,t_0) = \exp[(H_e+H_{\rm in}+H_{e\text{-in}})(t-t_0)/i\hbar]$, and $c_k(t)$ is given similarly.

Equation (13) can be calculated by the perturbation expansion of $c^{\dagger}_{k_1}(t') c_{k'_1}(t') c^{\dagger}_{k_2}(0) c_{k'_2}(0)$ with respect to $H_{e\text{-in}}$. In some of the expansion diagrams, the part including k_1 and k'_1 is linked to that including k_2 and k'_2 only by the input photon propagators, as shown in Fig. 2(a). In these diagrams, the output has a harmonic frequency of the input in spite of the spontaneous emission. Especially, the output with the same frequency as that of the input corresponds to the output signal of the device. This type of output is discussed in the next subsection, and a physical explanation is given in Sec. II D. In the diagrams other than those expressed by Fig. 2(a), the output has no relation to the input frequency. This corresponds to the noise in the device and is discussed in Sec. III C.

C. Output with the same frequency as input

The lowest-order term in which the output has the same frequency as the input is second order in $H_{e\text{-in}}$ shown in Fig. 2(b). Assuming the input photon number $N_{\rm in} \gg 1$, i.e., neglecting the spontaneous emission at the input port, the rate of output photon number obtained from the second-order perturbation is

$$\left\langle \frac{dN_{\rm out}}{dt} \right\rangle = \frac{2\pi}{\hbar^2} N_{\rm in} \delta(\omega_{\rm in}-\omega_{\rm out}) \times \left| \sum_{k_{\|}} \sum_{k_z k'_z} M^*_{\rm in}(k_z,k'_z) M_{\rm out}(k_z,k'_z) \times \int_{-\infty}^{\infty} [G_{k'}(\omega-\omega_{\rm in}) \sigma_z G_k(\omega)]^{--} \frac{d\omega}{2\pi} \right|^2, \tag{14}$$

where $G_k(\omega)$ is the matrix of the Keldysh-Green functions[6] given by

$$G_k(\omega) = \begin{bmatrix} G_k(\omega)^{--} & G_k(\omega)^{-+} \\ G_k(\omega)^{+-} & G_k(\omega)^{++} \end{bmatrix} \tag{15}$$

and

$$\sigma_z = \begin{bmatrix} 1 & 0 \\ 0 & -1 \end{bmatrix}. \tag{16}$$

The integrand in Eq. (14) comes from a bubble in Fig. 2(b), where $G_{k'}(\omega-\omega_{\rm in})$ and $G_k(\omega)$ interact via the matrix elements $M_{\rm in}$ and $M_{\rm out}$. The superscript "$--$" in Eq. (14) denotes the "$--$" element of the product of the matrices in the square brackets. The elements in Eq. (15) are written as

$$G_k(\omega)^{--} = \frac{f_k}{\hbar\omega-\mathcal{E}_k-i\Gamma_k} + \frac{1-f_k}{\hbar\omega-\mathcal{E}_k+i\Gamma_k}, \tag{17a}$$

$$G_k(\omega)^{-+} = \frac{f_k}{\hbar\omega-\mathcal{E}_k-i\Gamma_k} - \frac{f_k}{\hbar\omega-\mathcal{E}_k+i\Gamma_k}, \tag{17b}$$

$$G_k(\omega)^{+-} = -\frac{1-f_k}{\hbar\omega-\mathcal{E}_k-i\Gamma_k} + \frac{1-f_k}{\hbar\omega-\mathcal{E}_k+i\Gamma_k}, \tag{17c}$$

$$G_k(\omega)^{++} = -\frac{1-f_k}{\hbar\omega-\mathcal{E}_k-i\Gamma_k} - \frac{f_k}{\hbar\omega-\mathcal{E}_k+i\Gamma_k}, \tag{17d}$$

where f_k is the electron existing probability at k, which is determined by the emitter of the electron beam, and Γ_k is the imaginary part of the self-energy due to various scatterings expressed by $H_{\rm scattering}$ in Eq. (1). The real part of the self-energy is considered to be included in $\mathcal{E}_k$ hereafter. The self-energy is approximated to be independent of ω.

Substituting Eqs. (15)–(17) into Eq. (14), the rate of output photon number is calculated as (see the Appendix)

$$\left\langle \frac{dN_{\rm out}}{dt} \right\rangle = \frac{2\pi}{\hbar^2} N_{\rm in} \delta(\omega_{\rm in}-\omega_{\rm out}) \times \left| \sum_{k_{\|}} \sum_{k_z k'_z} \left[\frac{M^*_{\rm in}(k_z,k'_z) M_{\rm out}(k_z,k'_z)}{\mathcal{E}_k-\mathcal{E}_{k'}-\hbar\omega_{\rm in}+i\Gamma_k+i\Gamma_{k'}} + \frac{M_{\rm in}(k_z,k'_z) M^*_{\rm out}(k_z,k'_z)}{\mathcal{E}_k-\mathcal{E}_{k'}+\hbar\omega_{\rm in}-i\Gamma_k-i\Gamma_{k'}} \right] f_k \right|^2. \tag{18}$$

In this equation, the combinations of k_z and k'_z with the same signs are dominant and considered in the calculation below, because the matrix element in Eq. (6) is small for the com-

binations with different signs. The summations are transformed to integrals for the energies $\mathcal{E}_z$, $\mathcal{E}'_z$, and $\mathcal{E}_\parallel$ and are calculated by means of the contour integrals in the complex plane (see the Appendix). The result for k_z and $k'_z>0$ is

$$\left\langle \frac{dN_{\rm out}}{dt} \right\rangle = \frac{1}{2\pi\hbar^2} N_{\rm in}\delta(\omega_{\rm in}-\omega_{\rm out}) \left| \int_0^\infty d\mathcal{E}_\parallel \int_0^\infty d\mathcal{E}_z \frac{mS}{\pi\hbar^2} \times f(\mathcal{E}_z+\mathcal{E}_\parallel)[\mathfrak{M}(\mathcal{E}_z,\hbar\omega_{\rm in}-i\Gamma) - \mathfrak{M}^*(\mathcal{E}_z,-\hbar\omega_{\rm in}+i\Gamma)] \right|^2, \tag{19}$$

where $\Gamma=\Gamma_k+\Gamma_{k'}$ with Γ_k approximated to be independent of k, $f(\mathcal{E}_k)$ is the energy distribution for the electrons with $k_z>0$, and $\mathfrak{M}$ is given using Eq. (6) as

$$\begin{aligned} \mathfrak{M}(\mathcal{E}_z,\mathcal{E}) &= \left(\frac{L}{\hbar v_z(\mathcal{E}_z)}\right)^2 M_{\rm in}(k_z(\mathcal{E}_z),k_z(\mathcal{E}_z-\mathcal{E})) \\ &\quad \times M_{\rm out}(k_z(\mathcal{E}_z),k_z(\mathcal{E}_z-\mathcal{E})) \\ &\simeq \frac{e^2}{2\varepsilon}\sqrt{\frac{d_{\rm in}}{\hbar\omega_{\rm in}W_{\rm in}\ell_{\rm in}}}\sqrt{\frac{d_{\rm out}}{\hbar\omega_{\rm out}W_{\rm out}\ell_{\rm out}}} \\ &\quad \times M\left([k_z(\mathcal{E}_z)-k_z(\mathcal{E}_z-\mathcal{E})]\frac{d_{\rm in}}{2}\right) \\ &\quad \times M\left([k_z(\mathcal{E}_z)-k_z(\mathcal{E}_z-\mathcal{E})]\frac{d_{\rm out}}{2}\right) \\ &\quad \times e^{-i[k_z(\mathcal{E}_z)-k_z(\mathcal{E}_z-\mathcal{E})]D}. \end{aligned} \tag{20}$$

The summation for k_z and $k'_z<0$ is similarly calculated and is obtained to be zero (see the Appendix), indicating the natural fact that the output signal is emitted by the electron beam which traversed the input port at first.

The current of the electron beam is written as

$$I_0 = \sum_{k_z>0k_\parallel} ev_z f_k \frac{1}{L} = \frac{e}{2\pi\hbar}\int_0^\infty d\mathcal{E}_\parallel \int_0^\infty d\mathcal{E}_z \frac{mS}{\pi\hbar^2} f(\mathcal{E}_z+\mathcal{E}_\parallel). \tag{21}$$

If the distribution $f(\mathcal{E}_z+\mathcal{E}_\parallel)$, which depends on the structure of the electron emitter, is much narrower than other factors in the integral for $\mathcal{E}_z$ in Eq. (19), the rate of output photon number is approximated using Eq. (21) as

$$\left\langle \frac{dN_{\rm out}}{dt} \right\rangle \simeq 2\pi N_{\rm in}\frac{I_0^2}{e^2}\delta(\omega_{\rm in}-\omega_{\rm out})|\mathfrak{M}(\mathcal{E}_0,\hbar\omega_{\rm in}-i\Gamma) - \mathfrak{M}^*(\mathcal{E}_0,-\hbar\omega_{\rm in}+i\Gamma)|^2, \tag{22}$$

where $\mathcal{E}_0$ is the average kinetic energy of the electron beam in the z direction. The output photon rate is thus proportional to square of the current.

The higher-order perturbation must be analyzed for the discussion of the $N_{\rm in}$ dependence, as well as on the output with a harmonic frequency of the input. For the nth harmonic frequency, the $2n$th order perturbation calculation is at least necessary. Although the above analysis can be extended to higher-order perturbation, only the second-order perturbation is considered here, because the output characteristics in the small-input-signal case are discussed below.

In the above analysis, the spontaneous emission rate is calculated at the output port assuming the initial photon number is zero. If photons exist initially at the output port, stimulated emission also takes place. The rate of output photon number in this case is also calculated in the same manner as above. However, for an output with the same frequency as the input discussed above, the rates of the absorption and stimulated emission at the output port are the same, independent of the electron energy distribution. Therefore, the stimulated emission selective to the same frequency as the input does not appear. Conventional stimulated emission occurs with no relation to the input frequency.

D. Collective spontaneous emission

The output photon rate obtained in the previous subsection has only the same frequency as the input and is proportional to square of the current, as shown in Eq. (22). This is quite different from conventional spontaneous emission, in which the frequency is independent of input and the photon emission rate is proportional to the carrier density or current. A simple explanation is given for this difference by the collective spontaneous emission here.

For simplicity, a state $|\mathcal{E}_1,\mathcal{E}_2\rangle$ of an electron beam, in which the levels $\mathcal{E}_1$ and $\mathcal{E}_2$ have one electron each, is considered. By the interaction at the input port, this state emits and absorbs photons. For the purpose of seeing the phenomenon, it is enough to consider only the stimulated emission. The state after one-photon emission may be written as

$$C_0|\mathcal{E}_1,\mathcal{E}_2\rangle + C_1|\mathcal{E}_1-\hbar\omega_{\rm in},\mathcal{E}_2\rangle + C_1|\mathcal{E}_1,\mathcal{E}_2-\hbar\omega_{\rm in}\rangle. \tag{23}$$

The states for input and output photons are not written. This state then changes at the output port by the spontaneous emission. For example, the second term of Eq. (23) may change to

$$C'_0C_1|\mathcal{E}_1-\hbar\omega_{\rm in},\mathcal{E}_2\rangle + C'_1C_1|\mathcal{E}_1-\hbar\omega_{\rm in}-\hbar\omega_{\rm out},\mathcal{E}_2\rangle + C'_1C_1|\mathcal{E}_1-\hbar\omega_{\rm in},\mathcal{E}_2-\hbar\omega_{\rm out}\rangle. \tag{24}$$

If $\omega_{\rm out}\neq\omega_{\rm in}$, all terms generated from Eq. (23) express different states with each other. However, if $\omega_{\rm out}=\omega_{\rm in}$, the third term of Eq. (24) is equal to the term $C'_1C_1|\mathcal{E}_1-\hbar\omega_{\rm out},\mathcal{E}_2-\hbar\omega_{\rm in}\rangle$ which is generated from the third term of Eq. (23), and these two terms are superimposed in phase. The probability of the emission of one photon each at the input and output ports by these terms is $2|C'_1C_1|^2$ if $\omega_{\rm out}\neq\omega_{\rm in}$, while $4|C'_1C_1|^2$ if $\omega_{\rm out}=\omega_{\rm in}$. By extending this discussion to the many-electron system, the output photon rate has a peak at $\omega_{\rm out}=\omega_{\rm in}$ proportional to square of the carrier density or current. The origin of this phenomenon is the same as that of the superradiance from molecules.[7,8]

The above discussion can be applied similarly to the case of absorption instead of the stimulated emission at the input

port. The two terms in Eq. (22) in the previous subsection correspond to the stimulated emission and absorption cases. The difference of the signs of these two terms implies that the states generated by the emission and absorption at the input port are superimposed in antiphase.

E. Case of coherent input state

In the analysis of output photon rate in Secs. II B and II C, the photon number state is supposed for the input photon system as in Eq. (11). In this subsection, the coherent state

$$\overline{\rho_{\rm in}} = |\alpha\rangle\langle\alpha|, \tag{25}$$

with

$$|\alpha\rangle = \sum_{N_{\rm in}=0}^{\infty} \frac{\alpha^{N_{\rm in}}}{\sqrt{N_{\rm in}!}} e^{-|\alpha|^2/2} |N_{\rm in}\rangle, \tag{26}$$

is discussed for the initial state instead of Eq. (11). The rate of output photon number is calculated similarly to Sec. II C, if $|\alpha| \gg 1$. The result is expressed by changing $N_{\rm in}$ with $|\alpha|^2$ in Eq. (22), neglecting the factors time varying with frequency $2\omega_{\rm in}$. Since $|\alpha|^2$ approximately corresponds to the photon number of the coherent state in Eq. (26), this result means that the rate of output photon number is independent of whether the input state is the number state or the coherent state.

The expectation values of $a_{\rm out}$ and $a_{\rm out}^\dagger$ are nonzero in the coherent input case, in contrast to the number state. The output electric field, which is proportional to $a_{\rm out}^\dagger - a_{\rm out}$, has therefore a finite expectation value. For the coherent input state with the expectation value of the input electric field, $\mathrm{Re}[E_{\rm in} e^{-i\omega_{\rm in} t}]$, the expectation value of the output electric field is calculated in the first-order perturbation in $H_{e\text{-in}}$ and is obtained to be $\mathrm{Re}[E_{\rm out} e^{-i\omega_{\rm in} t}]$ with

$$E_{\rm out} \simeq [\mathfrak{M}(\mathcal{E}_0, \hbar\omega_{\rm in} + i\Gamma) - \mathfrak{M}^*(\mathcal{E}_0, -\hbar\omega_{\rm in} - i\Gamma)] \times \frac{I_0}{e}\left[\mathcal{P}\frac{1}{\omega_{\rm in} - \omega_{\rm out}} - i\pi\delta(\omega_{\rm in} - \omega_{\rm out})\right] E_{\rm in}, \tag{27}$$

where the term with the principal value denoted by $\mathcal{P}$ may vanish if the output electric field is integrated over the output angular frequency weighted with the output mode density. Equation (27) shows that the output electric field has a finite value with the same frequency as the input, if the input state is the coherent state.

III. OUTPUT CHARACTERISTICS

A. Output power

The power emitted at the output port is given by

$$P_{\rm out} = \int_{\omega_c - \Delta\omega/2}^{\omega_c + \Delta\omega/2} \left\langle \frac{dN_{\rm out}}{dt} \right\rangle \hbar\omega_{\rm out} \mathcal{D}(\omega_{\rm out}) d\omega_{\rm out}, \tag{28}$$

where ω_c and $\Delta\omega$ are the central frequency and the bandwidth of the used detector, and $\mathcal{D}(\omega_{\rm out})$ is the mode density given by

$$\mathcal{D}(\omega_{\rm out}) = \frac{\ell_{\rm out}}{2\pi}\sqrt{\varepsilon\mu}. \tag{29}$$

Using these equations and the relation

$$N_{\rm in} = \frac{\ell_{\rm in}\sqrt{\varepsilon\mu}}{\hbar\omega_{\rm in}} P_{\rm in} \tag{30}$$

between the input photon number $N_{\rm in}$ and the input power $P_{\rm in}$, the output power is obtained from Eq. (22) as

$$P_{\rm out} = \sqrt{\frac{\mu}{\varepsilon}}\frac{d_{\rm in}}{W_{\rm in}}\sqrt{\frac{\mu}{\varepsilon}}\frac{d_{\rm out}}{W_{\rm out}}\frac{I_0^2}{e^2} P_{\rm in} |\mathfrak{M}(\mathcal{E}_0, \hbar\omega_{\rm in} - i\Gamma) - \mathfrak{M}^*(\mathcal{E}_0, -\hbar\omega_{\rm in} + i\Gamma)|^2. \tag{31}$$

The following approximation can be made in $\mathfrak{M}$ given by Eqs. (20) and (6):

$$k_z(\mathcal{E}_0) - k_z(\mathcal{E}_0 - \mathcal{E}) \simeq \frac{\mathcal{E}}{\hbar v_0} - \frac{\mathcal{E}^2}{4\hbar v_0 \mathcal{E}_0}, \tag{32}$$

where $\mathcal{E} = \pm\hbar\omega_{\rm in} \mp i\Gamma$ and $v_0 = v_z(\mathcal{E}_0)$. $M_{\rm in}$ and $M_{\rm out}$ in Eq. (20) are approximated with this equation up to first order in $\mathcal{E}$, while the factor $e^{-i[k_z(\mathcal{E}_z) - k_z(\mathcal{E}_z - \mathcal{E})]D}$ is approximated up to second order to keep Eq. (31) finite. The output power is then approximated as

$$P_{\rm out} \simeq \sqrt{\frac{\mu}{\varepsilon}}\frac{d_{\rm in}}{W_{\rm in}}\sqrt{\frac{\mu}{\varepsilon}}\frac{d_{\rm out}}{W_{\rm out}} e^2 I_0^2 P_{\rm in} \left| \frac{1}{\hbar\omega_{\rm in}} M \times \left(\frac{(\hbar\omega_{\rm in} - i\Gamma)d_{\rm in}}{2\hbar v_0}\right) M\left(\frac{(\hbar\omega_{\rm in} - i\Gamma)d_{\rm out}}{2\hbar v_0}\right) \times \sin\left(\frac{(\hbar\omega_{\rm in} - i\Gamma)^2 D}{4\hbar v_0 \mathcal{E}_0}\right) \exp\left(-\frac{\Gamma D}{\hbar v_0}\right)\right|^2. \tag{33}$$

This equation is used in Sec. III B for a discussion of the influence of scattering.

The factors $\sqrt{\mu/\varepsilon}\, d_{\rm in}/W_{\rm in}$ and $\sqrt{\mu/\varepsilon}\, d_{\rm out}/W_{\rm out}$ in Eq. (33) are the characteristic impedances of the transmission lines at the input and output ports. These factors are resulted because the propagating EM waves are assumed. If standing waves excited by resonant cavities are assumed, ω_c and $\Delta\omega$ in Eq. (28) are regarded as the resonance angular frequency and the resonance width of the output cavity, and the above characteristic impedances are replaced by those of the input and output cavities to the electron beam. This result is obtained by using the vector potential and mode density of the standing waves in a cavity connected to outside,[9] instead of Eqs. (4) and (29). Since the characteristic impedances of resonant cavities are generally larger than those of the transmission lines, large output power can be obtained.

In the scattering free case ($\Gamma = 0$),

$$P_{\rm out} \simeq \sqrt{\frac{\mu}{\varepsilon}}\frac{d_{\rm in}}{W_{\rm in}}\sqrt{\frac{\mu}{\varepsilon}}\frac{d_{\rm out}}{W_{\rm out}} e^2 I_0^2 P_{\rm in} M^2\left(\frac{\omega_{\rm in} d_{\rm in}}{2v_0}\right) M^2\left(\frac{\omega_{\rm in} d_{\rm out}}{2v_0}\right) \times \left(\frac{1}{\hbar\omega_{\rm in}}\right)^2 \sin^2\left(\frac{\omega_{\rm in} D}{v_0}\frac{\hbar\omega_{\rm in}}{4\mathcal{E}_0}\right). \tag{34}$$

In the classical limit $\hbar\omega_{in}/\mathcal{E}_0 \to 0$, the third line of Eq. (34) reduces to $(\omega_{in}D/v_0)^2(1/4\mathcal{E}_0)^2$. The output power in this limit coincides with that of the classical analysis of the klystron vacuum tube for the small-signal case. Thus, the third line of Eq. (34) indicates the difference from the classical analysis. (In the classical theory,[1] the device operation is usually analyzed in the large signal case, resulting in the factor $J_1^2[(\omega_{in}D/v_0)(eE_{in}d_{in}/2\mathcal{E}_0)]/(eE_{in}d_{in})^2$ with the first-order Bessel function J_1, which approaches to the above factor in the small signal limit $(eE_{in}d_{in}/2\mathcal{E}_0 \to 0)$.) The above coincidence in the classical limit implies that the klystron vacuum tube in the microwave range is in the situation $\mathcal{E}_0 \gg \hbar\omega_{in} \gg \Gamma$.

The factors $\omega_{in}d_{in}/v_0$ and $\omega_{in}d_{out}/v_0$ included in Eq. (34) are the electron transit times at the input and output ports normalized by the period divided by 2π of the input frequency. In order to obtain high powers, these factors must be reduced, while the factor $\omega_{in}D/v_0$ must not be reduced. These conditions are the same as those in the classical results in the vacuum, except the size and electron energy are much smaller in a semiconductor. As an example, the power gain $P_{out}/P_{in} \simeq 21$ in Eq. (34) $(\Gamma=0)$ at $\omega_{in}d_{in}/2v_0 = \omega_{in}d_{out}/2v_0 = 0.5$, $\omega_{in}D/v_0 = 2$, $\sqrt{\mu/\varepsilon}\,d_{in}/W_{in} = \sqrt{\mu/\varepsilon}\,d_{out}/W_{out} = 100\ \Omega$ $(d_{in}/W_{in} = d_{out}/W_{out} = 1$ and the relative dielectric constant $=3.5)$, $\hbar\omega_{in} = 4$ meV $(f \simeq 1$ THz$) \ll \mathcal{E}_0 = 0.1$ eV $(v_0 \simeq 8 \times 10^7$ cm/sec with the effective mass $m = 0.05m_0)$, and $I_0 = 10$ mA. At these parameter values, the gaps of the input and output ports are $d_{in} = d_{out} \simeq 120$ nm. Larger gain will be obtained in the resonant cavity structures, as mentioned above. The degradation of the power gain due to the electron scattering is discussed in the next subsection. In the amplification obtained here, a part of the electron kinetic energy in the z direction is transferred to the output photon energy.

In Eq. (34), P_{out} increases with increasing D. This result arises from the different signs of the first and second terms of Eq. (22) or (31) discussed in the last part of Sec. II D. As shown in Eq. (20), these two terms are equal to each other except the phase factor $e^{-i[k_z(\mathcal{E}_z)-k_z(\mathcal{E}_z-\mathcal{E})]D}$. The difference of the phase factor increases with D, resulting in the increase of the output power. Thus, the mechanism generating the output includes two kinds of the interferences. One is the origin of the collective spontaneous emission discussed in Sec. II D, and the other is the destructive one discussed here. The combination of these interference approaches the velocity modulation and bunching of electrons[1] in the classical limit.

B. Influence of scattering

Figure 3 shows the power gain P_{out}/P_{in} calculated with Eq. (33) as a function of normalized energy broadening due to scattering, $\Gamma/\mathcal{E}_0$. The calculation results in Fig. 3 are normalized by Eq. (34) $(\Gamma=0)$ with the classical limit $\hbar\omega_{in}/\mathcal{E}_0 \to 0$. An example of the absolute value of the power gain with $\Gamma=0$ and the classical limit is given in the previous subsection. To extract the influence of scattering, the normalized transit times mentioned in the previous subsection are fixed as $\omega_{in}d_{in}/2v_0 = \omega_{in}d_{out}/2v_0 = 0.5$ and $\omega_{in}D/v_0 = 2$.

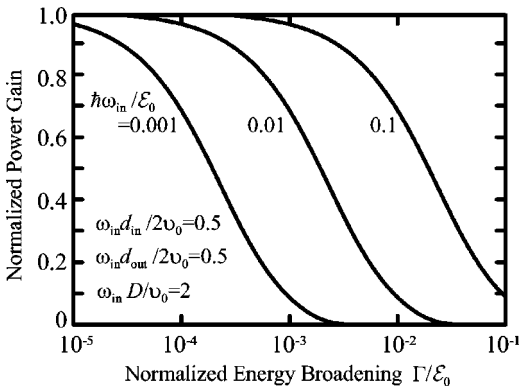

FIG. 3. Power gain normalized by the case with the energy broadening $\Gamma=0$ and $\hbar\omega_{in}/\mathcal{E}_0 \to 0$ (classical limit), as a function of $\Gamma/\mathcal{E}_0$, where $\mathcal{E}_0$ is the electron kinetic energy in the z direction.

As shown in Fig. 3, the power gain decreases with increasing energy broadening. Compared to the case with $\Gamma=0$ and $\hbar\omega_{in}/\mathcal{E}_0 \to 0$ (classical limit), the gain is much reduced at $\hbar\omega_{in} \lesssim \Gamma$. Γ is determined by various scattering mechanisms and is related to the phase breaking time[10] τ_ϕ as $\Gamma = \hbar/\tau_\phi$ or to the coherence length[11] ℓ_c as $\Gamma = \hbar v_0/\ell_c$. From the theoretical calculation of the hot electron scattering rate[12] and the estimation of the coherence length,[11] Γ is typically between about 1 meV and a few tens meV in compound semiconductors, and thus, $\hbar\omega_{in}$ must be approximately greater than this range, corresponding to a frequency f greater than sub-THz to a few tens THz. The high-frequency operation is not much influenced by the scattering, although the requirement that the normalized transit times at the input and output ports must be small enough becomes severe.

In addition to the limit in $\hbar\omega_{in}$, the input-output interval D is also restricted due to the influence of the scattering through the factor $e^{-\Gamma D/\hbar v_0}$ in Eq. (33). This factor disturbs the constructive interference discussed in Sec. II D. $\Gamma D/\hbar v_0 < 1$, i.e., $D <$ the coherence length, is required to suppress the influence of the scattering. However, D must not be too small to obtain a phase shift between the two terms in Eq. (31) as discussed in the last part of the previous subsection. To relax this restriction, insertion of a filtering potential structure just after the input port,[13] which eliminates the low-energy electrons generated by the stimulated emission at the input port, may be an effective method, although a precise design of the potential profile is necessary.

C. Signal-to-noise ratio

In the perturbation expansion mentioned in Sec. II B, diagrams other than those expressed by Fig. 2 give the output whose frequency has no relation with the input. These are the noise output of the device. The lowest-order term of these diagrams is zeroth order in $H_{e\text{-in}}$ obtained as

$$\left\langle \frac{dN_{out}}{dt} \right\rangle_{noise} = \frac{2}{\hbar} \sum_{k_\parallel k_z k_z'} |M_{out}(k_z, k_z')|^2 f_k(1-f_{k'}) \times \frac{\Gamma}{(\mathcal{E}_k - \mathcal{E}_{k'})^2 + \Gamma^2}. \quad (35)$$

Calculating similarly to Secs. II B and III A and, further, assuming $f_{k'} \ll 1$, i.e., low current density, the noise output power is approximated as

$$P_{\text{noise}} \simeq \frac{1}{4\pi^2}\sqrt{\frac{\mu}{\varepsilon}}\frac{d_{\text{out}}}{W_{\text{out}}} eI_0 \Delta\omega \int_{-\infty}^{\infty} M^2\left(\frac{\mathcal{E} d_{\text{out}}}{2\hbar v_0}\right) \times \frac{\Gamma}{(\mathcal{E}-\hbar\omega_{\text{out}})^2+\Gamma^2} d\mathcal{E} \simeq \frac{1}{4\pi}\sqrt{\frac{\mu}{\varepsilon}}\frac{d_{\text{out}}}{W_{\text{out}}} eI_0 \Delta\omega M^2\left(\frac{\omega_{\text{out}} d_{\text{out}}}{2v_0}\right). \quad (36)$$

In the final formula, Γ is assumed much smaller than the energy broadening of the factor M^2, which is a good approximation in the energy range discussed in Fig. 3. Since Eq. (36) is enough for the estimation of the noise power and the signal-to-noise ratio, higher-order perturbation terms including P_{in} are not discussed.

The signal-to-noise ratio defined by $S/N = P_{\text{out}}/P_{\text{noise}}$ is obtained from Eqs. (33) and (36) as

$$S/N \simeq 4\pi\sqrt{\frac{\mu}{\varepsilon}}\frac{d_{\text{in}}}{W_{\text{in}}}\frac{eI_0 P_{\text{in}}}{\Delta\omega}/M^2\left(\frac{\omega_{\text{in}} d_{\text{out}}}{2v_0}\right) \times \left|\frac{1}{\hbar\omega_{\text{in}}} M\left(\frac{(\hbar\omega_{\text{in}}-i\Gamma)d_{\text{in}}}{2\hbar v_0}\right) M\left(\frac{(\hbar\omega_{\text{in}}-i\Gamma)d_{\text{out}}}{2\hbar v_0}\right) \times \sin\left(\frac{(\hbar\omega_{\text{in}}-i\Gamma)^2 D}{4\hbar v_0 \mathcal{E}_0}\right)\exp\left(-\frac{\Gamma D}{\hbar v_0}\right)\right|^2. \quad (37)$$

As an example, $S/N = 3\times 10^{20}\times(P_{\text{in}}/\Delta f)$ for the same parameter values as in Sec. III A, P_{in} in watts, and $\Delta f = \Delta\omega/2\pi$ in hertz.

The influence of the scattering on S/N is just the same as that on the power gain shown in Fig. 3, as seen by normalizing S/N with the case of $\Gamma = 0$ and the classical limit $\hbar\omega_{\text{in}}/\mathcal{E}_0 \to 0$. Therefore, the device operation is limited to an input photon energy larger than the energy broadening due to the scattering and also to an input-output interval smaller than the electron coherence lenghth, with respect to both the power gain and signal-to-noise ratio.

IV. CONCLUSION

The interaction between a hot electron beam and electromagnetic waves was analyzed quantum mechanically in a semiconductor klystron structure. As a result of the collective spontaneous emission due to the interference between the specific many-electron states, the output photons have harmonic frequencies of the input, and the emission rate is proportional to square of the beam current. These characteristics are totally different from conventional spontaneous emission. The output power coincides with the result in the classical analysis in the low frequency limit. Due to the influence of scattering, the output power is much reduced for an input photon energy smaller than the electron energy broadening determined by the scattering and for an input-output interval larger than the electron coherence length. However, the output power is also small for a small interval, because of the destructive interference between the two states emitting and absorbing input photons. A potential filter located just after the input port, which eliminates low-energy states generated by the stimulated emission at the input port, may be effective to reduce the input-output interval, although a precise design of the potential profile is necessary.

ACKNOWLEDGMENTS

The author would like to acknowledge Professor Y. Suematsu, Professor Emeritus of the Tokyo Institute of Technology, for continuous encouragement. The author also thanks Professor K. Furuya and Professor S. Arai, Associate Professor Y. Miyamoto and Associate Professor M. Watanabe, and Dr. N. Machida for fruitful discussions. This work was supported by the Ministry of Education, Science, Sports and Culture by a scientific grand-in-aid.

APPENDIX A: CALCULATION OF THE OUTPUT PHOTON RATE

The calculation process to obtain Eq. (19) from Eq. (14) is described in this appendix. Using Eqs. (15)–(17) and a contour integral as in Ref. 14, the integral in Eq. (14) is calculated as

$$\int_{-\infty}^{\infty}[G_{k'}(\omega-\omega_{\text{in}})\sigma_z G_k(\omega)]^{--}\frac{d\omega}{2\pi} = \frac{f_k - f_{k'}}{\mathcal{E}_k - \mathcal{E}_{k'} - \hbar\omega_{\text{in}} + i\Gamma_k + i\Gamma_{k'}}. \quad (A1)$$

Substituting Eq. (A1) into Eq. (14), separating into two terms including f_k and $f_{k'}$, and exchanging the subscripts k and k' in the second term, Eq. (18) is obtained.

In the summation in Eq. (18), the combinations of k_z and k_z' with the same signs are dominant as mentioned in the text. The summation for k_z and $k_z' > 0$ is transformed to the integrals for energies as

$$\sum_{k_z k_z'} = \left(\frac{L}{2\pi}\right)^2 \int_0^{\infty}\frac{d\mathcal{E}_z}{\hbar v_z(\mathcal{E}_z)}\int_0^{\infty}\frac{d\mathcal{E}_z'}{\hbar v_z(\mathcal{E}_z')} = \left(\frac{L}{2\pi}\right)^2 \int_0^{\infty}\frac{d\mathcal{E}_z}{\hbar v_z(\mathcal{E}_z)}\int_{-\infty}^{\mathcal{E}_z}\frac{d\mathcal{E}}{\hbar v_z(\mathcal{E}_z-\mathcal{E})} \simeq \left(\frac{L}{2\pi}\right)^2 \int_0^{\infty}\frac{d\mathcal{E}_z}{\hbar^2 v_z^2(\mathcal{E}_z)}\int_{-\infty}^{\infty} d\mathcal{E}, \quad (A2)$$

where $\mathcal{E} = \mathcal{E}_z - \mathcal{E}_z'$. In the final formula of this equation, M_{in} and M_{out} in the integrals are assumed small enough at $\mathcal{E} \simeq \mathcal{E}_z \simeq \mathcal{E}_0$ compared to their maxima, where $\mathcal{E}_0$ is the average electron energy in the z direction determined by the distribution f_k. This condition is written as $(\hbar^2/2m)(2\pi/d_{\text{in}}$ or $d_{\text{out}})^2 \ll \mathcal{E}_0$ and is satisfied for the example of the parameter values given in Sec. III A.

Applying Eq. (A2) to Eq. (18), the first term in the absolute square of Eq. (18) is calculated as

$$\int_{-\infty}^{\infty} \frac{\mathfrak{M}(\mathcal{E}_z,\mathcal{E})}{\mathcal{E}-\hbar\omega_{\rm in}+i\Gamma} d\mathcal{E} = \oint_C \frac{\mathfrak{M}(\mathcal{E}_z,z)}{z-\hbar\omega_{\rm in}+i\Gamma} dz = -2\pi i \mathfrak{M}(\mathcal{E}_z,\hbar\omega_{\rm in}-i\Gamma), \quad \text{(A3)}$$

where C denotes the clockwise route consisting of the real axis from $-\infty$ to $+\infty$ and semicircle with an infinite radius in the lower half of the complex plane corresponding to $k_z(\mathcal{E}_z-z)>0$. The first equality of the above equation is satisfied because $|\mathfrak{M}(\mathcal{E}_z,z)|\to 0$ as $|z|\to 0$ in the lower half of the complex plane. The second term in the absolute square of Eq. (18) is calculated similarly with a contour integral in the upper half of the complex plane. Using these results, Eq. (19) is obtained.

The summation for k_z and $k_z'<0$ in Eq. (18) is transformed to the contour integrals with the same manner as above. However, due to the factor $e^{-i[k_z(\mathcal{E}_z)-k_z(\mathcal{E}_z-\mathcal{E})]D}$ in Eq. (20), the integral for the first term in Eq. (A3) must be calculated in the upper half plane because of the condition $|\mathfrak{M}(\mathcal{E}_z,z)|\to 0$ as $|z|\to 0$ for k_z and $k_z'<0$, and thus, the integral becomes zero. The second term is calculated in the lower half plane and also becomes zero.

*Electronic address: asada@pe.titech.ac.jp

[1] J. W. Gewartoski and H. A. Watson, *Principles of Electron Tubes* (Van Nostrand, Princeton, 1965).
[2] C. Becchi and G. Morpurgo, Phys. Rev. D **4**, 288 (1971).
[3] L. D. Favro and P. K. Kuo, Phys. Rev. A **7**, 866 (1973).
[4] H. J. Lipkin and M. Peshkin, Appl. Phys. Lett. **19**, 313 (1971).
[5] J. Kondo, J. Appl. Phys. **42**, 4458 (1971).
[6] E. M. Lifshitz and L. P. Pitaevskii, *Physical Kinetics* (Pergamon, New York, 1981).
[7] R. H. Dicke, Phys. Rev. **93**, 262 (1954).
[8] M. Sargent, M. O. Scully, and W. E. Lamb, Jr., *Laser Physics* (Addison-Wesley, Reading, MA, 1974).
[9] R. Lang, M. O. Scully, and W. E. Lamb, Jr., Phys. Rev. A **7**, 1788 (1973).
[10] S. Datta, J. Phys.: Condens. Matter **2**, 8023 (1990).
[11] M. Nagase, K. Furuya, and N. Machida, Jpn. J. Appl. Phys., Part 1 **40**, 3018 (2001).
[12] B. Y.-K. Hu and S. D. Sarma, Semicond. Sci. Technol. **7**, B305 (1992).
[13] M. Asada, Jpn. J. Appl. Phys., Part 2 **35**, L685 (1996).
[14] A. L. Fetter and J. D. Walecka, *Quantum Theory of Many-Particle Systems* (McGraw-Hill, New York, 1971), Chap. 4, p. 158.